CHALMERS
UNIVERSITY OF TECHNOLOGY

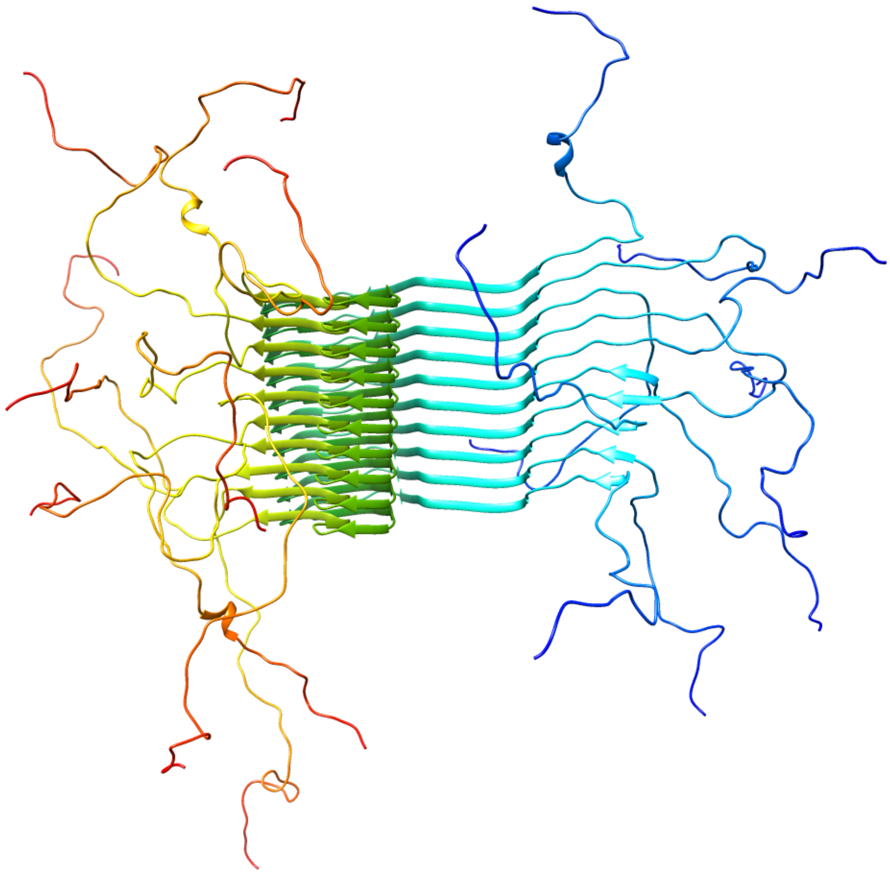

Catalytic Activity of α-Synuclein Amyloid Fibers

Master's thesis in Biotechnology

NIKITA REHNBERG

DEPARTMENT OF LIFE SCIENCES
CHALMERS UNIVERSITY OF TECHNOLOGY
Gothenburg, Sweden 2024
www.chalmers.se

Master's thesis 2024

Catalytic Activity of α-Synuclein Amyolid Fibers

NIKITA REHNBERG

CHALMERS
UNIVERSITY OF TECHNOLOGY

Department of Life Sciences
Division of Chemical Biology
Wittung-Stafshede Lab
Chalmers University of Technology
Gothenburg, Sweden 2024

Catalytic Activity of α-Synuclein Amyolid Fibers
NIKITA REHNBERG

Supervisor: Istvan Horvath, Life Scineces
Examiner: Pernilla Wittung-Stafshede, Life Sciences

Master's Thesis 2024
Department of Life Sciences
Division of Chemical Biology
Wittung-Stafshede Lab
Chalmers University of Technology
SE-412 96 Gothenburg
Telephone +46 31 772 1000

Cover: Atomic-resolution structure of α-Synuclein fibrils PDB ID: 2N0A.

Typeset in LaTeX
Printed by Chalmers Reproservice
Gothenburg, Sweden 2024

Catalytic activity of α-Synuclein amyolid fibers
NIKITA REHNBERG
Department of Life Sciences
Chalmers University of Technology

Abstract

Amyloid fibers play a significant role in neurodegenerative diseases such as Alzheimer's Disease (AD) and Parkinson's Disease (PD). They have for long been considered nonreactive dead-end products of protein aggregation. Recent research show that amyloid fibers, but not monomers, exhibit enzymatic catalytic activity in vitro. This project investigates the catalytic activity of α-Synuclein (aS) amyloid fibers. First, homogeneous aS amyloid fibers were made in a two-step seeding process and amyloids confirmed through ThT-fluorescence, far UV circular dichroism (CD) and atomic force microscopy (AFM). Then, an already established esterase activity assay, in vitro, was used to study ester bond cleavage of WT and A53T (disease-causing mutant) aS amyloid fibers. Another in vitro enzymatic assay was developed to study ATPase activity of WT, A53T and H50A (model of disease-causing mutants with altered residue 50) aS amyloid fibers. Results indicate that there is catalytic activity when aS amyloid fibers are incubated with both ester-bond and ATP substrates. However, the results are only qualitatively interpreted due to large variability in obtained kinetic parameters. To draw firm conclusions regarding the difference between the investigated aS mutants, additional experiments are needed.

Keywords: α-Synuclein, amyloid fibers, catalytic activity, Parkinson's Disease, esterase, ATP

Acknowledgements

I would like to express my sincere gratitude to Pernilla Wittung Stafshede and her invaluable guidance and support thought this project. Additionally, I am profoundly grateful to my supervisor, Istvan Horvath, for his mentorship and invaluable knowledge during this project. Special acknowledgement to Ranjeet Kumar for preparing all the protein I used. I am also grateful for the entire Wittung-Stafshede team for being really great coworkers always sharing their expertise and support.

I am thankful to all the individuals at the Division of Chemical Biology at the Department of Life Sciences at Chalmers University of Technology for making this project possible. Furthermore, I would like to express my gratitude to Area of Advance Health Engineering for their grant support which facilitated my research during the summer. Finally, I extend my appreciation to family and friends for always supporting me as well as all others who contributed in any way to the completion of this thesis.

Nikita Rehnberg, Gothenburg, February 2024

Contents

List of Figures

List of Tables

1
Introduction

Amyloid fibers play a significant role in various diseases, particularly in neurodegenerative disorders. Amyloid fibers refer to accumulations of aggregated or misfolded proteins that disrupt normal cellular function and contribute to disease. Alzheimer's disease (AD) ranks as the most prevalent neurodegenerative disorder, followed by Parkinson's disease (PD). With the global population expanding and life expectancy on the rise, the incidence of AD and PD is also increasing. [1]

Amyloid-β (Aβ) are amyloid forming peptides and one of the hallmarks of AD. [2] Lewy bodies, are insoluble accumulations of α-Synuclein (aS), and are one of the hallmarks for PD. [1]. Three recent publications has shown that amyloid fibers, including Aβ, aS and glucagon, can catalyze biologically relevant chemical reactions. Monomers under the same condition do not show catalytic activity. [2] [3] [4] Both Aβ and aS amyloid fibers have been shown to catalyse hydrolysis of a model substrate molecule, para-nitrophenyl acetate (pNPA). [2] [4] aS amyloid fibers have been demonstrated to also exhibit dephosphorylation activity using phosphoester para-nitrophenyl-orthophosphate (pNPP). [4] Glucagon is a protein that has a crucial role is regulating blood-glucose levels in the human body. Amyloid fibers of glucagon have been shown to have catalytic activity on various substrates, including dephosphorylation of adenosine triphosphate (ATP), a biologically relevant molecule. [3] Intriguingly, metabolomic studies have identified adenosine levels to increase when aS amyloid fibers are incubated in neuronal cells. [5] Considering amyloids to have functional properties is a novel and exciting perspective in this field of research.

1.1 Aim

The aim of the thesis was to investigate the catalytic activity of aS amyloid fibers for wild-type (WT) as well as histidine-50-alanine (H50A) and alanine-53-threonine (A53T) mutants. The investigation included preparation of amyloid fibers using seeded aggregation of aS. To confirm the amyloid fibers Thioflavin-T (ThT) fluorescence, circular dichroism (CD) and atomic force microscopy (AFM) was used. To study catalytic activity, two enzymatic assays were used and developed:

1. An already established esterase activity assay was used to study the enzymatic activity of two aS variants, WT and A53T.

2. A novel ATPase activity assay was designed and optimized to replace pNPP, used in an already established assay, with ATP, a biologically more relevant substrate. Developed for aS WT, A53T and H50A mutants to investigate the role of individual residues.

2
Theory

2.1 Parkinson's Disease

PD ranks as the second most prevalent neurodegenerative disorder. [1] At present, more than ten million people in the world are living with PD, and the number is estimated to rise to over 17 million in 2040. [6] The most common age for PD onset is between 55-65 years, although the disease likely begins its development long before symptoms manifest and are detectable. [7] While the cause of PD remains unclear, there are different clinical and pathological hallmarks of the disorder. Clinical signs demonstrate as symptoms such as tremors, slowness of movement, sleep problems, rigidity, pain and motor symptoms.

One pathological feature associated with PD is loss of dopaminergic neurons in the substantia nigra region of the brain. Dopamine plays an important role in voluntary movement, as well as other important brain functions such as mood regulation, reward processing, addiction and stress. [7] Research reveals that neurons are lost in other parts of the brain as well, such as in the locus ceruleus, nucleus basalis of Meynert, pedunculopontine nucleus, raphe nucleus, dorsal motor nucleus of the vagus, amygdala and the hypothalamus, underscoring the complexity of PD. Another characteristic feature of PD are presence of Lewy bodies, which are accumulations of folded proteins. aS folds into insoluble amyloid fibers forming the most abundant inclusion within Lewy bodies. These structures are primarily located in the brain where they disrupt dopaminergic neurons, but they have also been observed in other parts of the nervous system such as the spinal cord and various regions of the peripheral nervous system. Lewy body pathology is believed to progress over time and have been used as biological markers for PD. However, research continuously prove that the disorder is more complex than just Lewy body pathology. [1]

When aS folds into amyloid fibers it initially forms oligomers, which consist of approximately 2-100 aS monomers. aS oligomers have β-sheet structure with exposed hydrophobic regions making it possible for them to transport between neural cells or across the blood-brain barrier. Upon transport, they can promote folding of new amyloid fibers via elongation or secondary nucleation processes. aS oligomers could also be released from already formed aS amyloid fibers and they have been demonstrated to have immediate toxic effect on neuronal cells by disturbing their membranes. Consequently, aS oligomers are considered to be toxic species. [5] Animal model studies and analysis of blood and tissue samples from PD patients reveal metabolic changes as the disease progress. Energy metabolism, including metabolites associated with the tricarboxylic acid (TCA) cycle, has been shown to be affected in patients with PD. These changes in metabolites may arise from amyolid formation but are also speculated to be due to catalytic activity of amyloid fibers. [5]

PD is developed by a complicated interplay between genetic and environmental factors. PD can be sporadic but has also been linked to inherited genes. Six genes have been linked to PD; SNCA, LRRK2, VPS35, EIF4G1, DNAJC13, and CHCHD2. SNCA is coding for aS and mutations in this gene can cause disease linked amino acid substitutions, including A18T, A29S, A30P, E46K, H50Q, G51D, A53E and A53T. Multiplication of the SNCA gene locus can occur and leads to increased expression of aS which makes the protein more likely to form amyloid fibers. At present, there is no cure for PD. Current treatments focus on managing symptoms of the disease, such as increasing the amounts of dopamine. [1] PD is complex and it is difficult to understand causing relationships. An important focus for future research is to investigate the molecular process of neurodegeneration, aiming to understand the underlying molecular and cellular mechanisms. This includes unraveling why aS begins to fold into insoluble amyloid fibers.

2.2 α-Synuclein

aS is a 140 amino acid protein with a molecular weight of 14 kDa. The protein is intrinsically disordered, but can adopt different structures depending on its environment. Monomers lack regular structure, but when aggregated, aS adopts a β-sheet structure. When bound to lipid membranes, aS can adapt helical structure. [8] aS is abundant in the human brain, particularly found in in presynaptic nerve terminals in the substantia nigra region. [9]

The structure of aS is divided into three regions, figure 2.1 and figure 2.2, N-terminal, middle region and C-terminal. The N-terminal region, comprised of residues 1-60, contains four repeating sequences of eleven amino acids. This region creates amphipathic α-helices, making the region important for lipid membrane binding. [9] The middle region of aS, comprised of residues 61-95, is primarily hydrophobic. This region plays a significant role in the formation of amyloid structures. It contain the non-amyloid component (NAC) domain which is capable of forming cross-β structures. [10] The C-terminal region, comprised of residues 96 - 140, is disordered and contains many negatively charged amino acids, making it highly acidic. [8] [9]

MDVFMKGLSKAKEGVVAAAEKTKQGVAEAAGKTKEGVLYVGS	**N-terminal**
KTKEGVVHGVATVAEKTKEQVTNVGGAVVTGVTAVAQKTVEGAGSIAAATGFVKK	**Fiber core**
DQLGKNEEGAPQEGILEDMPVDPDNEAYEMPSEEGYQDYEPEA	**C-terminal**

Figure 2.1: aS amino acid sequence, N-terminal region in blue, middle region in green, C-terminal region in red, histidine-50 and alanine-53 in yellow. [4]

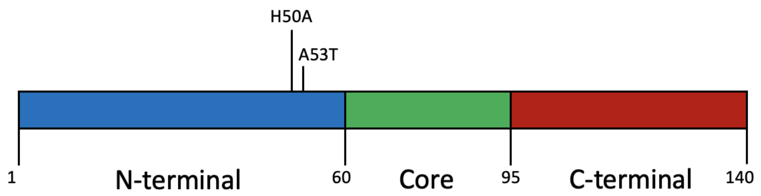

Figure 2.2: aS amino acid sequence, N-terminal region in blue, middle region in green, C-terminal region in red, H50A and disease linked A53T marked.

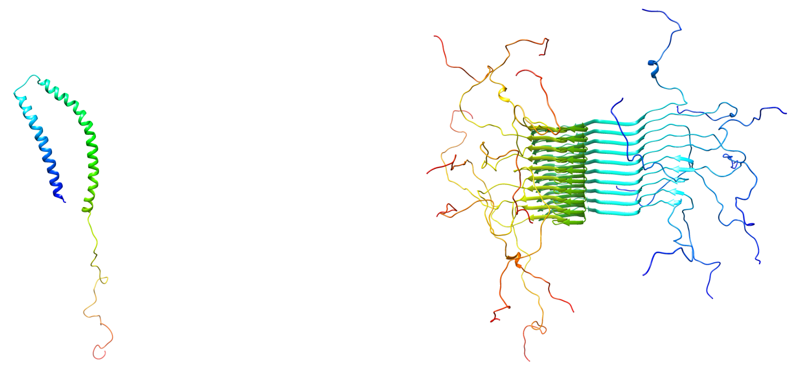

Figure 2.3: Left: human micelle-bound aS (PDB ID: 1XQ8). Right: structure of aS amyloid fiber as determined by solid state NMR (PDB ID: 2N0A).

2.3 Amyloid Fibers

Amyloids are peptide structures that have aggregated into insoluble structures characterized by highly organized arrays of β-sheet structures, known as cross-β structures. [11] Cross-β structures are made of of β-strands arranged perpendicularly to the fibril axis, assembled noncovaltently. [4]

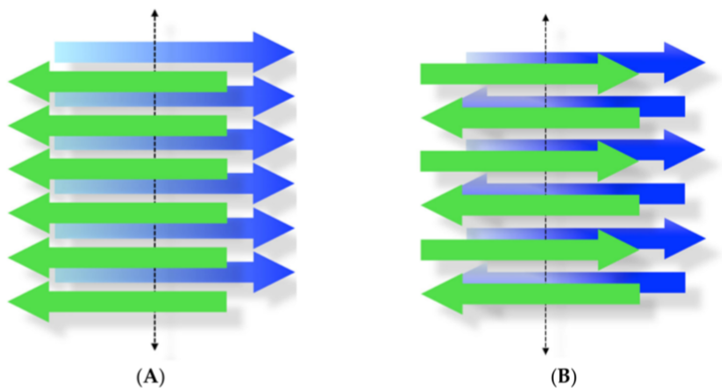

Figure 2.4: The most common cross-β structures in amyloid fibers. β-strands (blue and green) are arranged perpendicular to the fibrer axis (dotted black line). (A) parallel sheets and (B) anti-parallel sheets. [12]

Amyloid fiber formation can occur through different pathways. The initial step is primary nucleation, which involves spontaneous formation of oligomers from monomers in solution. This process is entirely dependent on the monomer concentration. Following primary nucleation, oligomers can grow and form amyloid fibers through different mechanisms, such as elongation, fragmentation or secondary nucleation. Elongation occurs when monomers are added to short fibers, resulting in the creation of amyloid fibers. Secondary nucleation, on the other hand, involves the catalysis of new nuclei formation by already-formed amyloid fibers on the surface of pre-existing amyloid fibers. Secondary nucleation is both monomer and amyloid fibers dependent. Fragmentation occurs when formed amyloid fibers break and serve as new starting products for the formation of new amyloid fibers. Figure 2.5 shows a typical amyloid fiber formation curve. All amyloid fibers formation processes occur at every phase in the curve, however, each phase is dominated by different processes. [13] In a typical amyloid formation curve, the lag phase is dominated by primary nucleation, monomers form intermediate oligomers. In the growth phase, the oligomers are rearranged and form cross-β structures which are thereafter formed into protofibrils. Finally, in the saturation phase, amyloids are formed. [13]

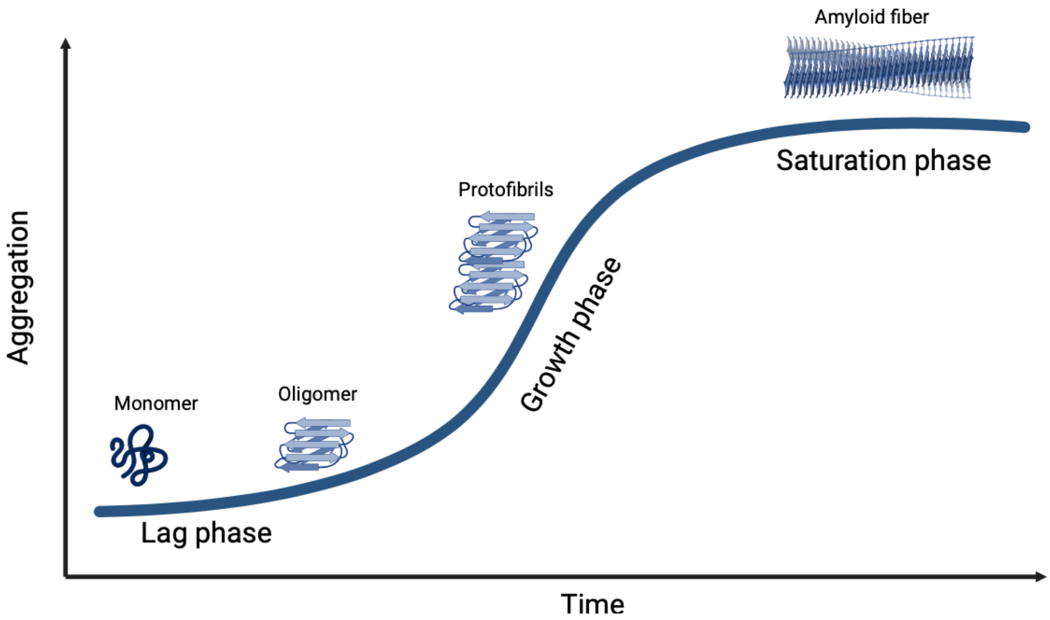

Figure 2.5: Amyloid fiber formation kinetics, including the different phases of amyloid fiber formation, lag phase, exponential growth phase and saturation phase. Created with BioRender.com.

2.4 Amyloid Fibers Catalyze Reactions in vitro

Recent reports have demonstrated that amyloid fibers catalyze biologically relevant chemical reactions, in vitro. [4] [2] [3] Aβ are amyloid fibers and one of the hallmarks of AD. It has been shown that Aβ amyloid fibers catalyze the hydrolysis of the model ester para-nitrophenyl acetate (pNPA) and of acetylthiocholine. Aβ has a hydrophilic region, containing nucleophilic amino acids such as lysine, serine, tyrosine and histidine, that are shown to have an important role in enzymatic active sites. [2]

Glucagon is a peptide hormone, that has an important role in regulating blood-glucose levels and in metabolic cascades affecting lipid metabolism. In certain conditions, glucagon can change into an amyloid structure. It has been demonstrated that glucagon amyloid fibers catalyze biologically relevant reactions such as esterolysis, lipid hydrolysis and dephosphorylation. Glucagon amyloid fibers catalyze dephosphorylation of ATP, a biologically relevant substrate. Catalytic activity for different glucagon mutants have been tested and when glucagon is lacking histidine at position 1 the catalytic activity is lower, suggesting a key role for histidine in catalytic performance. Moreover, histidine has been shown to activate nucleophilic attacks. Other nucleophilic amino acids such as lysine, threonine, serine and tyrosine can have similar roles in catalytic activities. [3]

WT aS amyloid fibers can catalyze the hydrolysis of the model substrate pNPA, converting it to pNP, as well as the dephosphorylation of the model pNPP, converting to pNP. Monomers under the same conditions do not exhibit any increase in either esterase or phosphatase catalytic activity. It has been observed that aS amyloid fibers, with a substitution of the amino acid H50A, are able to catalyze esterase activity to a similar extent as WT aS amyloid fibers. This substitution has effect on the phosphatase catalytic activity, indicating that the histidine residue may play a role in dephosphorylation. [4] To further investigate the catalytic activity of aS amyloid fibers, liquid chromatography-mass spectrometry (LC-MS) based metabolomic studies were done. aS amyloid fibers were incubated with neuronal SH-SY5Y cell lysates free of proteins and changes in metabolite levels were seen. In this study 63 metabolites were identified and four of them increased while 17 decreased. Intriguingly, adenosine was on of the four metabolites increased, after incubation with aS amyloid fibers. The remaining three metabolites that increase were 3-hydroxycapric acid, 2-pyrocatechuic acid and nicotinamide adenine dinucleotide (NAD). [5]

2.5 Enzyme Kinetics

Michaelis-Menten kinetics describe how reaction rate changes with substrate concentration in an enzyme-catalyzed reaction. Michaelis-Menten kinetics uses a simple model, involving one product and one substrate:

$$E + S \rightleftharpoons ES \rightleftharpoons EP \rightleftharpoons E + P$$

Assuming that chemical transformation of ES to EP is rate limiting, the following formula is derived:

$$E + S \rightleftharpoons ES \rightarrow E + P$$

The turnover number, k_{cat}, is the rate-determining conversion of substrate to product. It gives information of the rate of product formation under optimum conditions, when the enzyme is saturated. k_{cat} can be interpreted as the time it takes for one enzyme molecule to "turn over" one substrate molecule [11]. Michaelis-Menten kinetics can be investigated experimentally and valuable parameters can be obtained. A Michaelis-Menten graph, figure 3, is described by the following equation:

$$v = \frac{V_{max} \times [S]}{K_m + [S]}$$

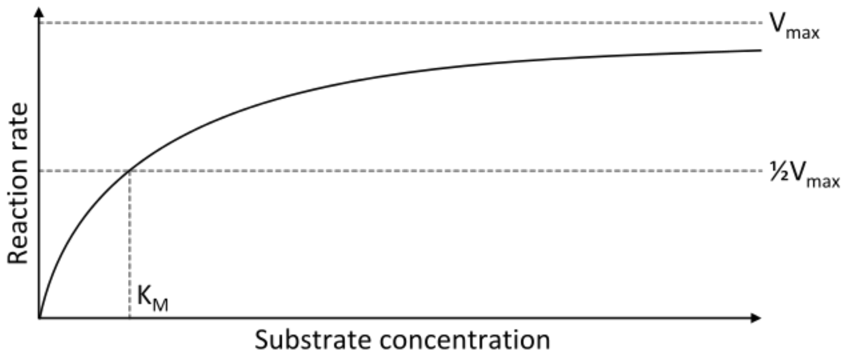

Figure 2.6: Michaelis-Menten plot of reaction rate (v) as a function of initial substrate concentration, including parameters K_m and V_{max} [11].

The y-axis represents velocity, the rate at which the reaction proceeds. The x-axis represents initial substrate concentration, [S]. If the enzyme concentration is held constant, a saturation plateau will appear at high concentrations of substrate. At this plateau, the reaction velocity reaches its maximum, which is denoted as V_{max}. At V_{max}, all enzymes are present in the form of enzyme-substrate complexes. V_{max} provides valuable information about the upper limit of the reaction velocity, given a specific amount of enzyme.

The Michaelis-Menten constant, K_m, refers to the substrate concentration required for the reaction to reach half of V_{max}. When K_m is compared between different enzyme-substrate reactions, it gives valuable information on enzyme-substrate affinity. A high K_m indicates lower affinity, while a low K_m indicates higher affinity [14]. Another valuable parameter is $\varepsilon = k_{cat}/K_m$ which provides information on the enzyme efficiency and specificity. It behaves as a second-order rate constant. k_{cat} can be derived from $V_{max} = k_{cat}[E_t]$, where $[E_t]$ is the total amount of enzyme added [11].

2.6 Analytic Methods

2.6.1 Thioflavin-T Fluorescence

ThT fluorescence is a useful tool for monitoring the formation of amyloid structures. ThT is a fluorescent benzothiazole dye that produces a wavelength shift, with excitation and emission maxima at 440 nm and 490 nm respectively, and an increase in fluorescence emission when it binds to cross-β structures. Non-bound ThT emits very weak fluorescence, with excitation and emission maxima at 350 nm and 440 nm respectively. This sensitivity and specificity makes it a useful method for studying amyloid formation. [15]

2.6.2 Circular Dichroism

CD is an absorption spectroscopy method, based on the differential absorption of left and right polarised light, that provides information about the secondary structure of proteins. A monochromatic light of a single wavelength is passed though a polarizer where it becomes linearly polarised, oscillating in one plane. Thereafter, the polarised light is passed though a quarter phase filter making it circularly polarised, consisting of two components, one rotating clockwise (right polarised) and the other is rotating counter-clockwise (left polarised). A sample is then bombarded with the circular polarised light and the absorption of left and right polarised light will be different if our sample contains chiral molecules. Amino acids are chiral, they exist in L-form and D-form. Depending on the secondary structure of a protein, the chiral arrangement will be different and thus give rise to different CD spectra. Figure 2.7 shows characteristic CD spectra in the far-UV region from α-helix, β-sheet or random coil structures.

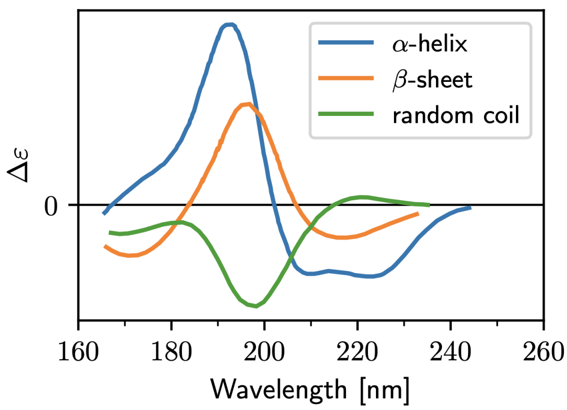

Figure 2.7: CD Reference graph showing spectra for full α-helix structure (blue), full β-sheet structure (orange) and lack of regular structure (green) [16].

CD data can be presented in either differential absorption (ΔA) or ellipticity (θ mdeg). If the data is in absorption units, equation 2.1 can be used to calculate the molar differential extinction coefficient $\Delta\epsilon$. Where l is the cuvette path length and C is the molar protein concentration. [17]

$$\Delta\epsilon = \frac{A_L - A_R}{l * C} \tag{2.1}$$

Equation 2.2 provides a numerical relationship between ellipticity (θ mdeg) and differential absorbance.[17]

$$\theta(mdeg) = 180ln10\frac{\Delta A}{4\pi} = 32.98\Delta A \tag{2.2}$$

Equation 2.3 normalizes the observed θ_{obs} into mean molar residue ellipticity θ_{MRE} to reduce the samples dependency on path length and molar protein concentrations to make samples comparable. [17]

$$\theta_{MRE} = 100\frac{\theta_{obs}}{C * l * N} \tag{2.3}$$

2.6.3 Atomic Force Microscopy

AFM is a high resolution imaging method to study topography and mechanical properties of amyloid fibers. A sharp metal tip, attached to a cantilever, is placed slightly over a sample. A laser beam is directed to, and reflected by, the cantilever. An array of small photodiodes is placed to detect changes in position of the reflected laser beam. The sharp metal tip is moved over the sample and the detected changes in position of the laser beam is converted to imagines [14]. The imagines are collected and provide information of the sample topography and morphology on a nanometer scale [18]. This information can help to characterise and determine whether the correct aS amyloid fibers have been made.

2.6.4 Esterase Activity Assay

To investigate esterase activity of aS amyloid fibers pNPA can be used as a model substrate. Here, an ester bond (C-O) is being cleaved and the formed product pNP can be detected via absorption at 410 nm. [4] Figure 2.8 shows the chemical reaction probed in this project.

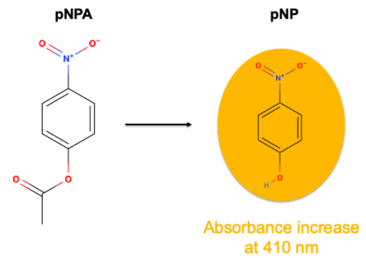

Figure 2.8: Chemical reactions probed in esterase assay. Esterase activity, hydrolysis of pNPA to pNP. Formation of pNP can be detected via absorption at 410 nm.

2.6.5 ATPase Activity Assay

ATP is a molecule used to store energy at a cellular level. ATP is a nucleoside triphosphate, consisting of adenine, a ribose sugar and three bonded in series phosphate groups. The phosphate groups are linked though phosphodiester bonds which are high energy bonds because of electronegative charges creating a repelling force between the phosphate groups. To release energy, ATP is hydrolyzed into either adenosin diphosphate (ADP) or adenosine monophosohate (AMP) and free inorganic monophosphate or pryophosphate groups are released. [14] In addition, glucagon fibers have been shown to catalyze dephosphorylation of ATP. [3] WT and H50A aS amyloid fibers have phosphatase activity using model substrate pNPP. [4]

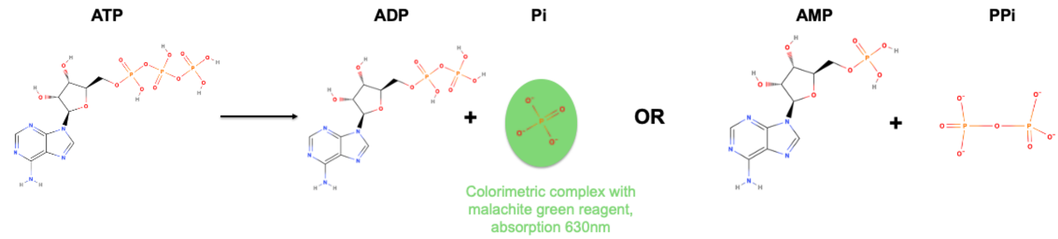

Figure 2.9: Chemical reactions probed in ATP assay. ATPase activity, dephosphorylation of ATP to ADP or AMP. Malachite green can only be used for detection of monophosphate, not pyrophosphate, meaning that AMP can not be detected by this method.

Figure 2.9 shows the reaction probed in this assay. Malachite green reagent can be used to quantify monophosphate cleaved from ATP. Monophosphate reacts with ammonium molybdate and forms phosphomolybdate, which reacts with malachite green and forms detectable colorimetric complex which can be detected via at absorption at 630 nm. However, this method does not detect pyrophosphate, if ATP is cleaved directly into AMP. [19]

3

Methods

3.1 Protein Expression and Purification

The protein expression and purification was done by R. Kumar according to a previously published protocol. [20] WT, A53T and H50A aS protein were expressed in *Escherichia coli* grown in LB broth. Anion exchange and size exclusion were used for protein purification. The buffer used was Tris-buffered saline (TBS) containing 0.15 M NaCl and 0.050 M Tris-HCl at pH 7.6 and 25°C. The protein was stored at -80°C until used in experiments. [20]

3.2 Preparation of α-Synuclein Amyloid Fibers

3.2.1 Gel Filtration

Fresh aS amyloid fibers were prepared before each assay experiment. Monomeric aS-protein was taken from -80°C freezer. Before starting amyloid formation, gel filtration was preformed to remove potential aggregates in the aS-monomer samples. For the gel filtration a Superdex 75 10/300 column and TBS buffer was used.

3.2.2 Thioflavin-T Fluorescence

The gel filtrated WT, A53T and H50A aS monomers were aggregated using a two step aggregating process. Firstly, the protein was incubated under agitation with glass beads for 3-4 days. The incubation was performed at 37°C in a plate reader (BMG Labtech, Fluostar Optima) and 0.0165 mM ThT was added and ThT-fluorescence was used to monitor the formation of amyloid structures. After 3-4 days the aggregated aS-fibers, were frozen using liquid nitrogen and then aliqouted and stored at -80°C.

Secondly, the aggregated aS amyloid fibers were added to newly gel filtrated aS-monomers, with starting seed concentrations 2.8 μM, 1 μM, 4.3 μM for WT, A53T and H50A respectively, approximately 1-5% of protein starting concentration. The mixture was incubated in the plate reader for 24 h, at 37°C, using ThT-florescence to monitor amyloid formation. After amyloid formation, the samples were centrifuged for 30 min at 135000 g to remove remaining monomeric protein. The pellet, aggregated aS amyloid fibers, was then diluted back into TBS buffer. Absorbance at 280 nm was used to estimate the fiber concentration.

3.2.3 Circular Dichroism

WT, A53T and H50A aS amyloid fibers and monomers were diluted to approximately 5-10 μM. CD was then used, between 190-250 nm, to confirm β-sheet secondary structure for aS amyloid fibers and the lack of secondary structures, random coil, for aS monomers. β-sheet structure was characterized by a positive band near 198 nm and negative band near 215 nm. Random coil structure was characterized by a strong band just below 200 nm and a very weak band at 217 nm.

3.2.4 Atomic Force Microscopy

AFM was used to study topography and mechanical properties of WT, A53T and H50A aS amyloid fibers. The aS amyloid fibers were diluted in filtered milli-Q water to between 5-10 μM. Thereafter, 200 μl of the sample was placed for 10 min in RT on a mica plate. Water was removed using filter paper and the sample was washed with filtered milli-Q water three times. There upon, the sample was dried using nitrogen steam. To obtain the images NTEGRA Prima setup, gold-coated single-crystal silicon cantilever (NT-MDT, NSG01, spring constant of 5.1 N/m) and resonance frequency of 180 kHz in tapping mode was used. Scan rate of 0.5 Hz was used for the images. WSxM 5.0 software was used to analyze the images.

3.3 Colorimetric Enzyme Assays

One already establish esterase activity assay was used to study the enzymatic esterase activity of aggregated WT and A53T aS amyloid fibers. [4] A new assay was developed and optimized to investigate the dephosphorylation activity of WT, A53T and H50A aS amyloid fibers on ATP molecules.

3.3.1 Esterase Activity Assay

The purpose of the esterase assay was to investigate catalyzed hydrolysis of the model ester para-Nitrophenyl acetate (pNPA) to para-Nitrophenyl (pNP) product. Here, an ester bond (C-O) is being cleaved, figure 2.8 shows the chemical reaction probed in this assay.

Sample mixtures of aS amyloid fibers, WT and A53T respectively, were mixed with pNPA substrate in 0.05 M phosphate buffer, pH 7.4. For all assays, a fresh stock solution, kept on ice, containing 18 mg of 4-nitrophenyl acetate (pNPA)(Sigma Aldrich) diluted in 500 ul acetonitrile (Sigma Aldrich) was prepared. The stock solution was then diluted and mixed with WT and A53T respectively aS amyloid fibers according to table A.1 resp. A.2. The same mixtures were made for WT and A53T aS monomers to confirm that aS monomers do not show catalytic activity. Blank samples were made in the same way but aS protein was omitted from the mixtures and instead TBS-buffer was used.
The sample mixtures were then incubated in 96-well half area transparent-bottom plates with nonbinding surface (Corning) using plate reader incubator (Fluorostar

Optima; BMG Labtech). Absorbance at 410 nm was measured every 3 min, for 60 min. To convert the measured absorbance values to pNP concentration the extrication coefficient 7500 $M^{-1}cm^{-1}$ was used. The obtained values were fitted to Michaelis-Menten kinetic curves and K_m and V_{max} values were calculated. For these calculations, values from the first 30 min of the experiment was used.

3.3.2 ATPase Activity Assay

The purpose of the ATPase assay was to investigate the dephosphorylation of ATP molecules, from ATP to ADP. In this reaction a P-O bond is being cleaved, figure 2.9 shows the chemical reaction probed in this assay.

For this assay, malachite green dye was used to quantify the monophosphate cleaved from ATP. Monophosphate reacts with ammonium molybdate and forms phosphomolybdate, which reacts with malachite green and forms a colorimetric complex that can be detected by absorption at 630 nm. Sample mixtures of WT, A53T and H50A aS amyloid fibers were mixed with ATP substrate in reaction buffer, containing 20 mM Tris, 1 mM EGTA and 5 mM MgSO4 at pH7.5. For all assays, a fresh stock solution, kept on ice, containing 0.01 g ATP (Sigma Aldrich) in 1000 μl reaction buffer, was used to obtain an ATP concentration of 20 mM.

The stock solution was then diluted and mixed with the freshly prepared WT, A53T and H50A aS amyloid fibers according to table A.3, A.4 resp. A.5. The same mixtures were made for WT, A53T and H50A aS monomers to confirm that aS monomers do not show catalytic activity. Blank samples were made in the same way but aS protein was omitted from the mixtures and instead TBS-buffer was used. A standard curve, using standard solution in phosphate assay kit (Sigma Aldrich), was prepared and treated in the same was as the samples. The standard curve was used to relate absorption values at 630 nm to monophosphate concentration.

The sample mixtures were then incubated in 384-well black with transparent-bottom plates with nonbinding surface (Corning), using plate reader incubator (Fluorostar Optima; BMG Labtech). At specific time points, according to table A.3, the reactions were stopped by adding malachite green reagent from phosphate assay kit (Sigma Aldrich), A.4 and A.5 and then incubated in RT for 30 min for color development. Thereafter, absorbance at 630 nm was measured. The obtained absorbance values, at the specific time points, where translated into monophosphate concentration using the prepared standard curve. At time zero the monophosphate concentration was assumed to be zero. Then Michaelis-Menten kinetic curves where fitted and K_m and V_{max} values were calculated.

4

Results

4.1 Thioflavin-T Fluorescence

The curves in figure 4.1 represents normalized ThT-fluorescence for WT, A53T and H50A aS amyloid fibers. In all cases, the curves indicate that aS monomers have aggregated into amyloid fibers.

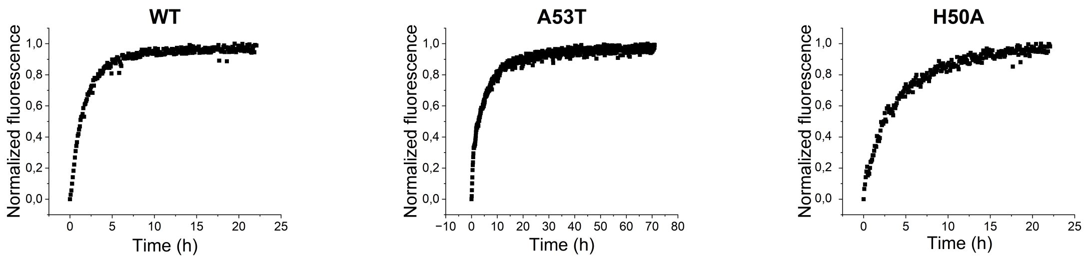

Figure 4.1: Normalized ThT-fluorescence curves for aggregated WT, A53T and H50A aS amyloid fibers.

4.2 Circular Dichroism

Figure 4.2 shows the CD spectra between 190-250 nm for 10 μM WT, A53T and H50A aS amyloid fibers and, 10 μM WT and A53T aS monomers. To confirm formation of aS amyloid fibers the graphs in figure 4.2 were compared to figure 2.7. β-sheet structure was characterized by a positive band near 198 nm and a negative band near 215 nm. Random coil structure was characterized by a strong band just below 200 nm and a very weak band at 217 nm. Confirming the secondary β-sheet structure for the prepared aS amyloid fibers and the lack of secondary structures for the aS monomers. CD measurements for H50A aS amyloid fibers and monomers could be repeated for more firm conclusion regarding secondary structure.

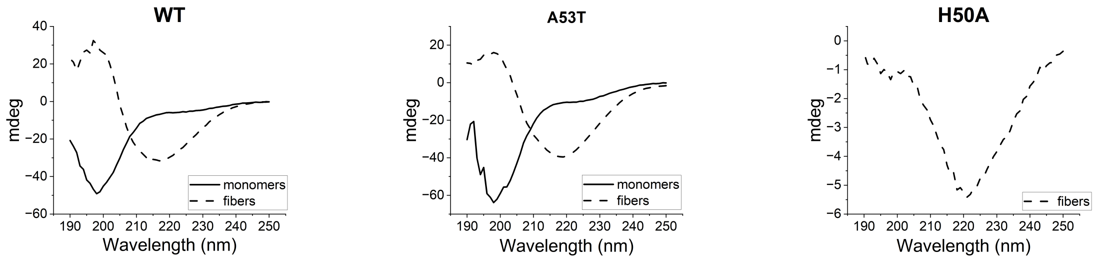

Figure 4.2: CD spectra between 190-250 nm for 10 μM WT, A53T and H50A aS amyloid fibers and, 10 μM WT and A53T aS monomers.

4.3 Atomic Force Microscopy

Figure 4.3 presents AFM images of WT, A53T and H50A aS amyloid fibers. The aS amyloid fibers, all variants, have long, unbranched structures. Figure 4.4 shows height profiles of aS amyloid fibers to be around 7.5 nm, 7.0 nm and 4.5 nm for WT, A53T and H50A respectively.

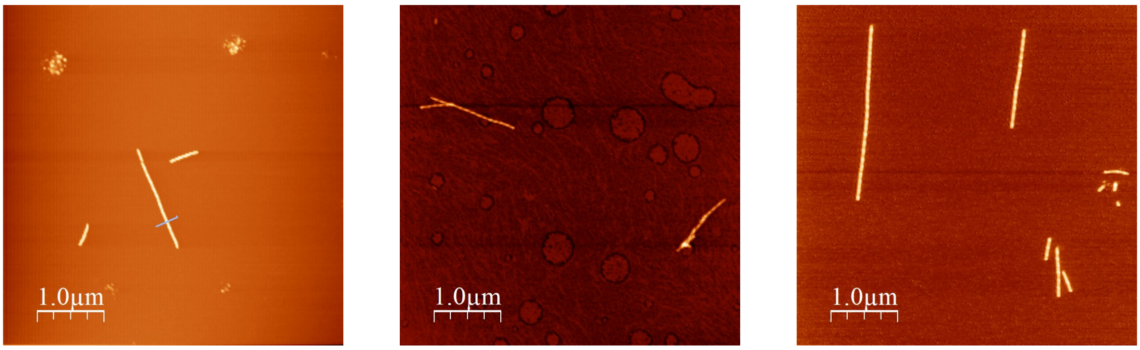

Figure 4.3: AFM images. Left: 10 μM WT aS amyloid fibers. Middle: 10 μM A53T aS amyloid fibers. Right: 10 μM H50A aS amyloid fibers.

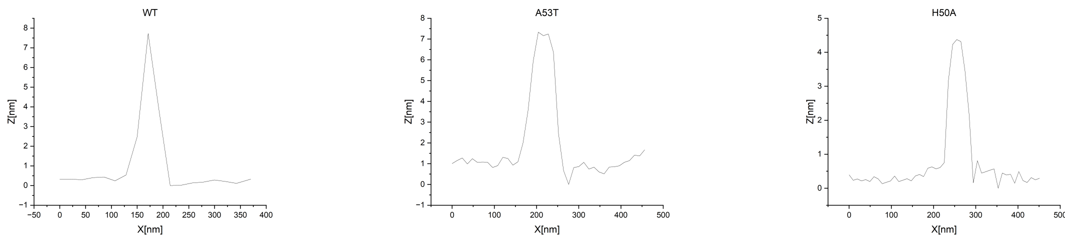

Figure 4.4: Height profiles of aS amyloid fibers seen in 4.3. Left: 10 μM WT aS amyloid fiber height. Middle: 10 μM A53T aS amyloid fiber height. Right: 10 μM H50A aS amyloid fiber height.

4.4 Esterase activity assay

In total, ten esterase activity assays were done, with varied parameters according to tables A.1 and A.2. Presented in figure 4.5 are results from two separate esterase activity assay experiments, one for WT aS amyloid fibers and the other for A53T aS amyloid fibers. Table 4.1 provides K_m and V_{max} values for WT and A53T aS amyloid fibers respectively. Additional results are presented in figures A.1 and A.2.

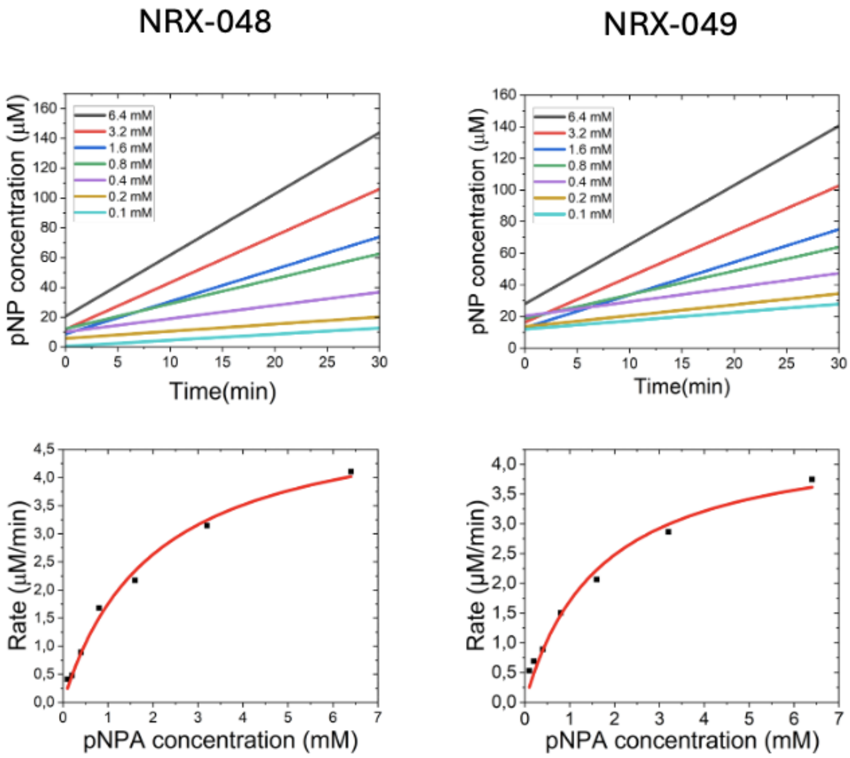

Figure 4.5: Esterase activity. Top left and right: 20 μM WT aS amyloid fibers and 20 μM A53T aS amyloid fibers, respectively, incubated with different inital concentrations of pNPA substrate. pNP product detected and traced via absorption at 410 nm. Bottom left and right: reaction rates (μM/min) plotted against initial pNPA concentration (mM) and Michaelis-Menten fitted curves.

Experiment ID	**aS variant**	**Km [mM]**	**Vmax [μM/min]**
NRX-048	WT	2.0	5.3
NRX-049	A53T	1.7	4.6

Table 4.1: Michaelis-Menten kinetic parameters, K_m and V_{max}, using pNPA substrate and 20 μM WT and A53T aS amyloid fibers, respectively.

4.5 ATPase activity assay

In total, twenty-four ATPase activity assays were done, with varied parameters according to tables A.3, A.4 and A.5. Figure 4.6 shows two graphs where A53T aS amyloid fibers and H50A aS amyloid fibers, respectively, were compared to aS monomers of the same variant, after incubation with ATP substrate. In both cases, more monophosphate product is formed when ATP is incubated with aS amyloid fibers than with aS monomers. Experiments could be repeated using WT aS amyloid fibers and monomers for a stronger conclusion.

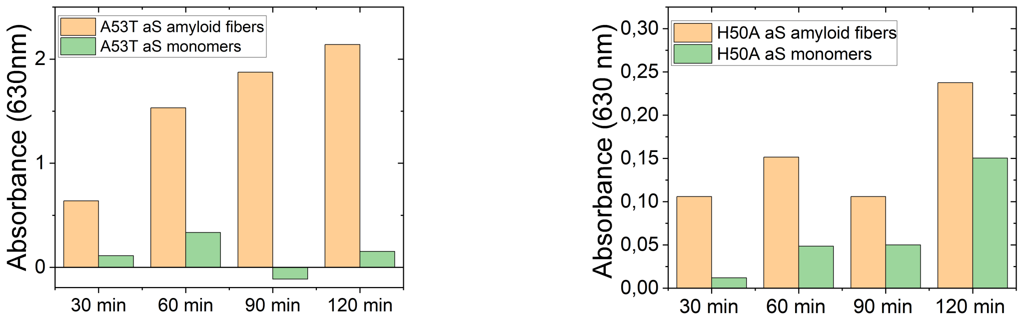

Figure 4.6: Left: ATP incubated with A53T aS amyloid fibers and monomers. Right: ATP incubated with H50A aS amyloid fibers and monomers. Both reactions stopped at different time-points, seen on x-axis, monophosphate detected via absorbance at 630 nm.

Presented in figure 4.7 are results from three separate ATPase activity assay experiments, for WT, A53T and H50A aS amyloid fibers. Table 4.2 provides K_m and V_{max} values for WT, A53T and H50A aS amyloid fibers, respectively. Additional results are presented in figures A.3, A.4 and A.5.

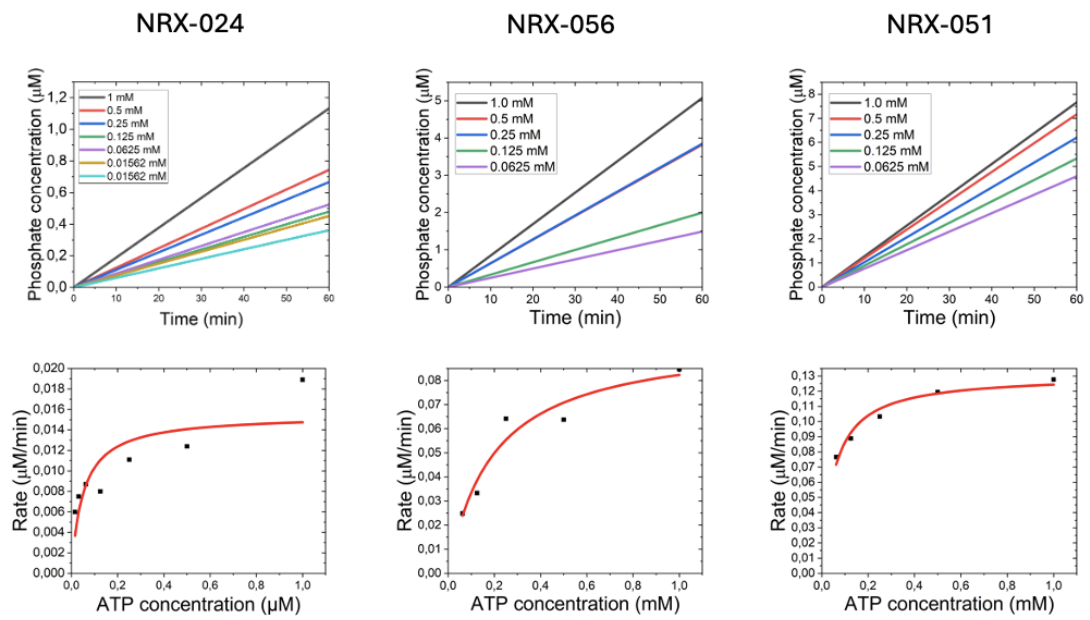

Figure 4.7: ATPase activity. Top left, middle and right: 40 μM WT, A53T and H50A, respectively, aS amyloid fibers incubated with different initial concentrations of ATP substrate. Monophosphate product detected via malachite green regent and absorption at 630 nm. Monophosphate concentration is assumed to be zero at timepoint zero. Bottom left, middle and right: reaction rates (μM/min) plotted against initial ATP concentration (mM) and Michaelis-Menten fitted curves.

Experiment ID	**aS variant**	**Km [mM]**	**Vmax [μM/min]**
NRX-024	WT	0.05	0.02
NRX-056	A53T	0.20	0.10
NRX-051	H50A	0.05	0,13

Table 4.2: Michaelis-Menten kinetic parameters, K_m and V_{max}, using ATP substrate and 40 μM WT, A53T and H50A aS amyloid fibers, respectively.

5

Discussion and Conclusion

5.1 Discussion

To explore esterase activity pNPA substrate was used, wherein an ester bond is cleaved and the formed pNP product was detected. Figure 4.5 shows result graphs from two separate experiments, one using WT aS amyloid fibers, the other using A53T aS amyloid fibers. When aS amyloid fibers, both variants, were incubated with a higher initial pNPA concentration, the reaction rate was faster. This is visualized in top left and right graphs, figure 4.5, where time (min) is plotted against pNP concentration (μM). Michaelis-Menten fitted curves, reaction rate (μM/min) plotted against initial pNPA concentration (mM), are shown in bottom right and left graphs, figure 4.5. Table 4.1 provides Michaelis-Menten kinetic parameters, K_m and V_{max}, for both the experiments. A higher K_m indicates lower affinity between substrate and enzyme. Due to time limitation, no experiments were done using aS monomers, but relying on previous publications, WT aS amyloid fibers do not exhibit catalytic activity.

Esterase activity of WT aS amyloid fibers has previously been reported to have K_m value 4.3 $\pm$ 2.5 mM. [4] The K_m value 2.013 mM, from this experiment, table 4.1, falls within the range of the previously reported values. However, A.1, provides two additional esterase activity experiments with K_m values of 14.76 mM and 0.63 mM which gives a broad range of values and more replicates would be needed for a firm conclusion regarding differences between aS mutants. Table 4.1 also provides a K_m value of 1.69 mM for aS A53T variant, indicating higher catalytic esterase activity for aS A53T amyloid fibers compared to aS WT amyloid fibers. A53T is a disease linked mutant, making it interesting to investigate. However, A.1, provides two additional replicate experiments with K_m values 87.85 mM and 5.83 mM, these are dispersed values and more replicates would be needed for a firm conclusion regarding differences between aS variants. Previous publications have investigated WT and H50A aS variants, and proven them to have significant similar esterase catalytic activity. Other publications, have proven glucagon amyloid fibers to exhibit similar activity but amyloid-β amyloid fibers to have less activity than aS amyloid fibers.

Previous work have been published on dephosphorylation activity of aS amyloid fibers, using a model substrate pNPP, showing catalytic activity of aS WT amyloid fibers but notably much less activity for H50A aS amyloid fibers. This could indicate that the histidine residue might play a crucial role for dephosphorylation activity of aS amyloid fibers. Monomers of both variants, WT and H50A, did not show catalytic activity. This study was aimed to further investigate dephosphorylation activity of aS amyloid fibers but instead of using a model substrate pNPP, a real biological substrate, ATP, was used and three aS variants, WT, A53T and H50A, were investigated. Figure 4.7 shows graphs from three separately preformed experiments using three different aS mutants WT, A53T and H50A. All ATPase activity Michaelis-Menten fitted curves are poor and cannot be used to make comparisons between aS variants. Reported Michaelis-Menten parameters in table 4.2 should not be used to draw firm conclusions, they can only be qualitatively interpreted. K_m values were 0.05035 mM, 0.1956 mM and 0.052 mM respectively for WT, A53T and H50A mutants. Previous published work, using model substrate pNPP, showed less dephosphorylation activity for H50A than for WT and a similar outcome could be predicted when ATP was used as a substrate. When looking at the graphs in figure 4.7 and their corresponding Michaelis-Menten parameters in table 4.2, it does not corroborate with WT having a higher dephosphorylation activity than both A53T and H50A variants, in fact, the opposite is indicated. However, when comparing those results to replicate experiment results provided in figure A.3, A.4 and A.5 with corresponding kinetic parameters in table A.3, A.4 and A.5, a broad range of values are obtained and more replicates would be needed for a conclusion. As previously stated, ATPase activity kinetic parameters should not be used to compare between aS mutants due to poor Michaelis-Menten fits.

Intriguingly, ion-pair chromatography findings, conducted by S. Sharma and A. Chabes at Umeå University, reveal separate detection of ATP, ADP or AMP. The results suggest that when WT aS amyloid fibers are incubated with ATP substrate, incubated by I. Horvath, AMP appears to be the predominant product formed, with ADP formation small in comparison. The ion-pair chromatography experiment needs to be repeated for firm conclusions. These results are interesting since the malachite green detection method used in this study, only detects monophosphate, meaning if pyrophosphate is cleaved of ATP and AMP is formed, it is not detected. The method in this study could be developed to also detect pyrophosphate by using pyrophsohatase enzyme that specifically cleaves pyrophosphate into monophosphate. Other published results, prove adenosine to be one of four increased metabolites when aS amyloid fibers were incubated in neuronal cells. Indicating that dephosphorylation of ATP might occur in the presents of aS amyloid fibers. Future work could also include investigating catalytic activity of other increased metabolites from the metabolomic study, such as NAD. Another interesting study would be to identify potential binding cites on amyloid fibers for substrates.

5.2 Conclusion

In conclusion, aS amyloid fibers exhibit both esterase and ATPase catalytic activity. Based on the results from this study it is difficult to draw firm conclusions regarding differences between the activity of aS variants WT, A53T and H50A.

Bibliography

1. Kalia L and Lang A. Parkinson's disease. The Lancet 2015;386:896–912. DOI: https://doi.org/10.1016/S0140-6736(14)61393-3.
2. Arad E, Baruch Leshem A, Rapaport H, and Jelinek R. β-Amyloid fibrils catalyze neurotransmitter degradation. ACS Nano 2021;1:908–22. DOI: https://doi.org/10.1016/j.checat.2021.07.005.
3. Arad E, Yosefi G, Kolusheva S, Bitton R, Rapaport H, and Jelinek R. Native Glucagon Amyloids Catalyze Key Metabolic Reactions. ACS Nano 2022;16:12889–99. DOI: https://doi.org/10.1021/acsnano.2c05166.
4. Horvath I and Wittung-Stafshede P. Amyloid Fibers of a-Synuclein Catalyze Chemical Reactions. ACS Chemical Neuroscience 2023;14:603–8. DOI: https://doi.org/10.1021/acschemneuro.2c00799.
5. Horvath I, Mohamed K, Kumar R, and Wittung-Stafshede P. Amyloids of α-Synuclein Promote Chemical Transformations of Neuronal Cell Metabolites. Int. J. Mol. Sci. 2023;24:12849. DOI: 10.3390/ijms241612849.
6. Dorsey E, Sherer T, Okun M, and Bloem B. The Emerging Evidence of the Parkinson Pandemic. J Parkinsons Dis 2018;1:3–8. DOI: 10.3233/JPD-181474.
7. Chinta D and Julie K. Andersen J. Dopaminergic neurons. The International Journal of Biochemistry and Cell Biology 2005;37:942–6. DOI: https://doi.org/10.1016/j.biocel.2004.09.009.
8. Emamzadeh F. Alpha-synuclein structure, functions, and interactions. J Res Med Sci. 2016;21:NA. DOI: doi:10.4103/1735-1995.181989.
9. Breydo L, Wu J, and Uversky V. synuclein misfolding and Parkinson's disease. Biochim Biophys Acta. 2012;1822:261–85. DOI: https://doi.org/10.1016/j.bbadis.2011.10.002.
10. Gallardo J, Escalona-Noguero C, and Sot B. Role of a-Synuclein Regions in Nucleation and Elongation of Amyloid Fiber Assembly. ACS Chemical Neuroscience 2020;11:872–9. DOI: https://doi.org/10.1021/acschemneuro.9b00527.
11. Appling D, Anthony-Cahill S, and Mathews C. Biochemistry Concepts and Connectios. Pearson Education Limited, 2016.
12. Duran-Meza E.and Diaz-Espinoza R. Amyloids as Novel Synthetic Hydrolases. Int. J. Mol. Sci. 2021;22:9166. DOI: https://doi.org/10.3390/ijms22179166.
13. Meisl G, Kirkegaard J, Arosio P, and al. et. Molecular mechanisms of protein aggregation from global fitting of kinetic models. Nat Protoc 2016;11:252–72. DOI: https://doi.org/10.1038/nprot.2016.010.

14. Mikkelsen S. Bioanalytical Chemistry. John Wiley and Sons, Incorporated, 2016.
15. Hudson S, Ecroyd H, Kee T, and Carver J. The thioflavin T fluorescence assay for amyloid fibril detection can be biased by the presence of exogenous compounds. Protein Misfolding, Prions and Amyloid 2009;276:5960–72. DOI: https://doi.org/10.1111/j.1742-4658.2009.07307.x.
16. Gustafsson-Agrenius T. A quantum chemical study of electronic circular dichroism in alanine oligopeptides. KTH Royal Institute of Technology Stockholm, Sweden 2018:8.
17. Kelly S, Jess T, and Price N. How to study proteins by circular dichroism. Biochimica et Biophysica Acta (BBA) - Proteins and Proteomics 2005;1751:119–39. DOI: https://doi.org/10.1016/j.bbapap.2005.06.005.
18. Martin Y. Method for imaging sidewalls by atomic force microscopy. Applied Physics Letters 1994;64:2498–500. DOI: 10.1063/1.111578[doi].
19. Carter S and DW. K. Inorganic phosphate assay with malachite green: An improvement and evaluation. Journal of Biochemical and Biophysical Methods 1982;7:7–13. DOI: https://doi.org/10.1016/0165-022X(82)90031-8.
20. Werner T, Kumar R, Horvath I, and al et. Abundant fish protein inhibits α-synuclein amyloid formation. Nature Scientific Reports 2018;8:XXX. DOI: 10.1038/s41598-018-23850-0.

A

Appendix 1

This section contains tables over all assays, esterase and ATP, with aS variants, WT, A53T and H50A, at different substrate concentrations. As well as additional result graphs from colorimetric enzyme assays.

A.1 Esterase Activity Assay Results

A.1.1 WT alpha-Synuclein Amyloid Fibers

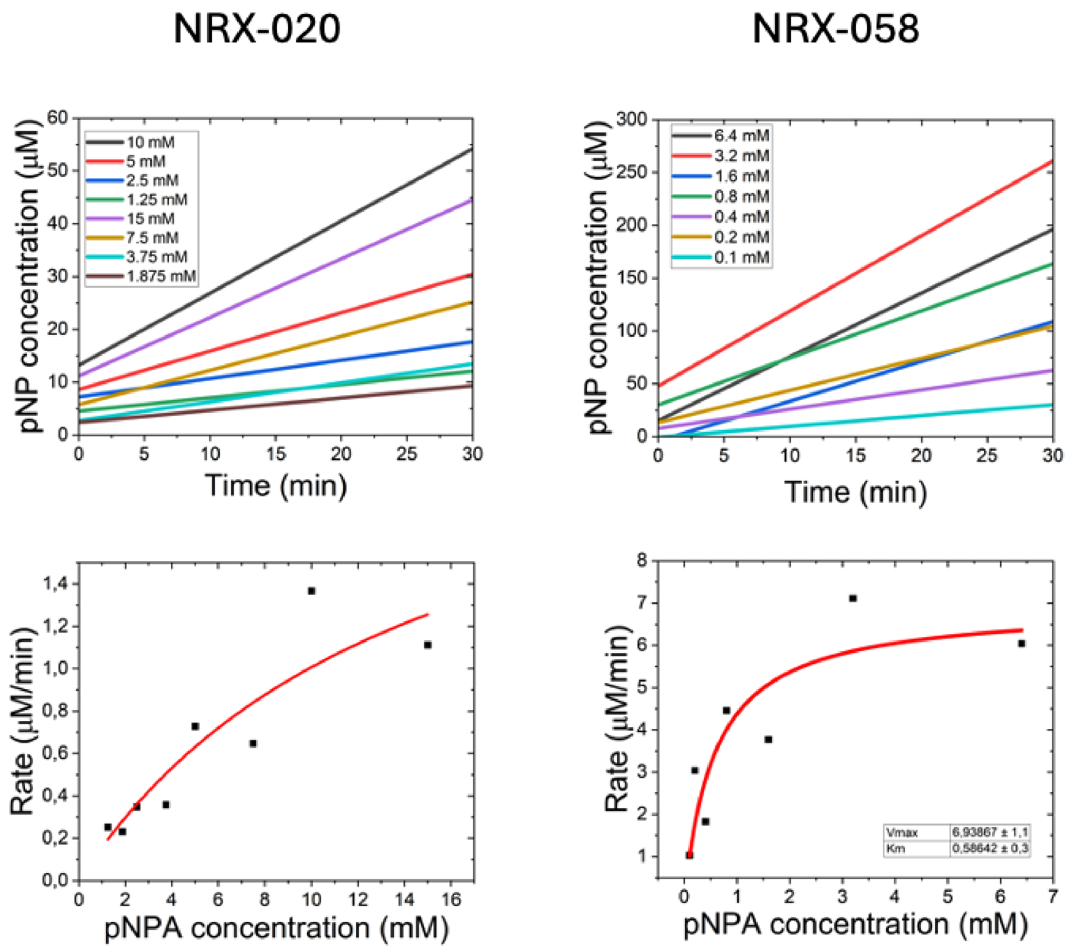

Figure A.1: Esterase activity results of aS WT amyloids.

Experiment ID	pNPA [mM]	aS-fiber [μM]	Km [mM]	Vmax [μM/min]
NRX-020	1.874 - 15, 1.25 - 10	10	14.76	2.49
NRX-058	0.1 - 6.4	20	0.63	6.85

Table A.1: Esterase activity assay mixtures containing WT aS-fibers mixed with pNPA substrate in PI-buffer. Half dilutions were done between provided pNPA concentrations.

A.1.2 A53T alpha-Synuclein Amyloid Fibers

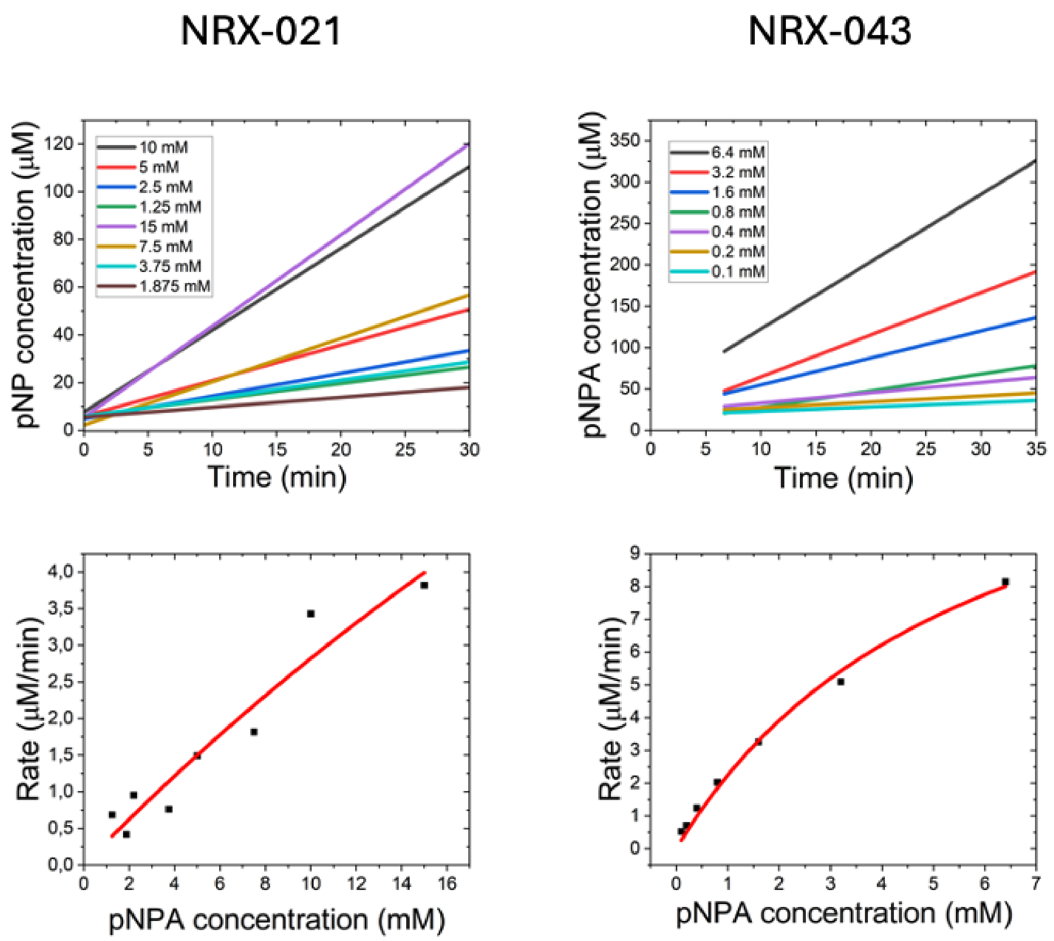

Figure A.2: Esterase activity results of aS A53T amyloids.

Experiment ID	pNPA [mM]	aS-fiber [μM]	Km [mM]	Vmax [μM/min]
NRX-021	1.874 - 15, 1.25 - 10	10	87.85	28.01
NRX-043	0.1 - 6.4	20	5.82	15.29

Table A.2: Esterase activity assay mixtures containing A53T aS-fibers mixed with pNPA substrate in PI-buffer. Half dilutions were done between provided pNPA concentrations.

A.2 ATPase Activity Assay Results

A.2.1 WT alpha-Synuclein Amyloid Fibers

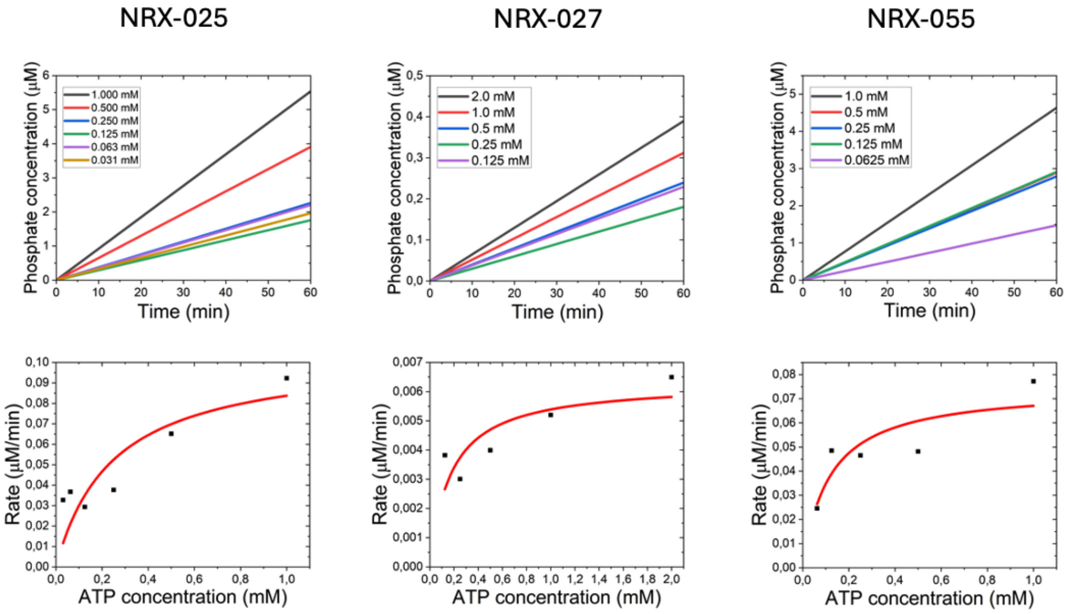

Figure A.3: ATPase activity results of aS WT amyloid fibers.

Experiment ID	ATP [mM]	aS-fiber [μM]	Km [mM]	Vmax [μM/min]
NRX-025	0.015625 - 1	40	0.248	0.1044
NRX-027	0.125 - 2	20	0.176	0.0063
NRX-055	0.0625 - 1	40	0.115	0.0748

Table A.3: ATPase activity assay mixtures containing WT aS-fibers mixed with ATP substrate in reaction-buffer. Half dilutions were done between provided ATP concentrations.

A.2.2 A53T alpha-Synuclein Amyloid Fibers

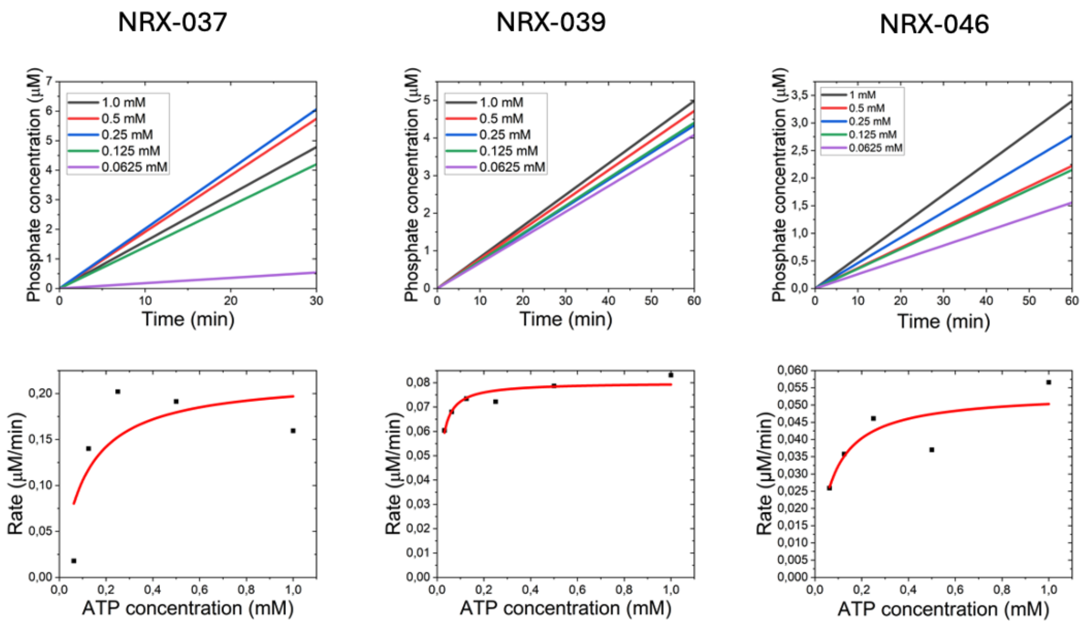

Figure A.4: ATPase activity results of aS A53T amyloids.

Experiment ID	ATP [mM]	aS-fiber [μM]	Km [mM]	Vmax [μM/min]
NRX-037	0.0625 - 1	40	0.1071	0.2179
NRX-039	0.03125 - 0.5	40	0.011	0.0801
NRX-046	0.03125 - 0.5	40	0.0657	0.0536

Table A.4: ATPase activity assay mixtures containing A53T aS-fibers mixed with ATP substrate in reaction-buffer. Half dilutions were done between provided ATP concentrations.

A.2.3 H50A alpha-Synuclein Amyloid Fibers

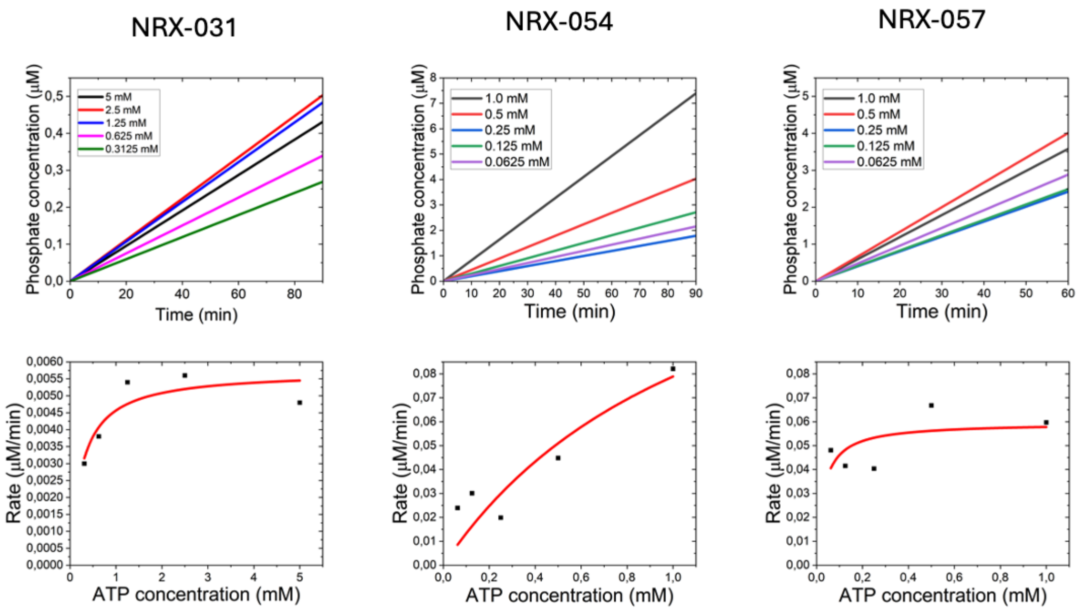

Figure A.5: ATPase activity results of aS H50A amyloids.

Experiment ID	ATP [mM]	aS-fiber [μM]	Km [mM]	Vmax [μM/min]
NRX-031	0.625 - 10	40	0.2549	0.00573
NRX-054	0.0625 - 1	40	1,21	0,1744
NRX-057	0.0625 - 1	40	0.02903	0.0595

Table A.5: ATPase activity assay mixtures containing H50A aS-fibers mixed with ATP substrate in reaction-buffer. Half dilutions were done between provided ATP concentrations.

DEPARTMENT OF SOME SUBJECT OR TECHNOLOGY
CHALMERS UNIVERSITY OF TECHNOLOGY
Gothenburg, Sweden
www.chalmers.se

CHALMERS
UNIVERSITY OF TECHNOLOGY